Balance of mechanical forces drives endothelial gap formation and may facilitate cancer and immune-cell extravasation

Escribano, Jorge; Chen, Michelle B.; Moeendarbary, Emad; Cao, Xuan; Shenoy, Vivek; Garcia-Aznar, Jose Manuel; Kamm, Roger D.; Spill, Fabian

DOI:
10.1371/journal.pcbi.1006395

PLOS COMPUTATIONAL BIOLOGY

RESEARCH ARTICLE

Balance of mechanical forces drives endothelial gap formation and may facilitate cancer and immune-cell extravasation

Jorge Escribano[1,2], Michelle B. Chen[2,3], Emad Moeendarbary[2,4], Xuan Cao[5], Vivek Shenoy[5], Jose Manuel Garcia-Aznar[1]*, Roger D. Kamm[2,6,7]*, Fabian Spill[6,8]*

1 Department of Mechanical Engineering, University of Zaragoza, Zaragoza, Spain, **2** Department of Biological Engineering, Massachusetts Institute of Technology, Cambridge, Massachusetts, United States of America, **3** Department of Bioengineering, Stanford University, Stanford, California, United States of America, **4** Department of Mechanical Engineering, University College London, London, United Kingdom, **5** Department of Materials Science and Engineering, University of Pennsylvania, Philadelphia, Pennsylvania, United States of America, **6** Department of Mechanical Engineering, Massachusetts Institute of Technology, Cambridge, Massachusetts, United States of America, **7** BioSystems and Micromechanics (BioSyM), Singapore-MIT Alliance for Research and Technology, Singapore, Singapore, **8** School of Mathematics, University of Birmingham, Birmingham, United Kingdom

* jmgaraz@unizar.es (JMGA); rdkamm@mit.edu (RDK); f.spill@bham.ac.uk (FS)

OPEN ACCESS

Citation: Escribano J, Chen MB, Moeendarbary E, Cao X, Shenoy V, Garcia-Aznar JM, et al. (2019) Balance of mechanical forces drives endothelial gap formation and may facilitate cancer and immune-cell extravasation. PLoS Comput Biol 15(5): e1006395. https://doi.org/10.1371/journal.pcbi.1006395

Editor: Andrew D. McCulloch, University of California San Diego, UNITED STATES

Received: July 19, 2018

Accepted: December 10, 2018

Published: May 2, 2019

Data Availability Statement: All relevant data are within the paper and its Supporting Information files. The code used to implement the model and produce the computational results shown is available on Github: https://github.com/Escribs/Endothelial-monlayer.

Funding: This study was funded by the National Cancer Institute grant numbers U01 CA202177 and U01 CA177799 to RDK, the Spanish Ministry of Economy and Competitiveness (FPI: BES-2013-

Abstract

The formation of gaps in the endothelium is a crucial process underlying both cancer and immune cell extravasation, contributing to the functioning of the immune system during infection, the unfavorable development of chronic inflammation and tumor metastasis. Here, we present a stochastic-mechanical multiscale model of an endothelial cell monolayer and show that the dynamic nature of the endothelium leads to spontaneous gap formation, even without intervention from the transmigrating cells. These gaps preferentially appear at the vertices between three endothelial cells, as opposed to the border between two cells. We quantify the frequency and lifetime of these gaps, and validate our predictions experimentally. Interestingly, we find experimentally that cancer cells also preferentially extravasate at vertices, even when they first arrest on borders. This suggests that extravasating cells, rather than initially signaling to the endothelium, might exploit the autonomously forming gaps in the endothelium to initiate transmigration.

Author summary

Transmigration of immune cells into and out of the blood vessels is a crucial process for the functioning of the immune system during infections and acute inflammations, and aberrant transmigration may contribute to chronic inflammations. Likewise, cancer metastasis critically depends on intra-and extravasation of cancer cells through the endothelium. While much research investigated the role of immune or cancer cells in signaling to the endothelium, facilitating effective transmigration, and some work uncovered a role of passive mechanical properties such as stiffness during transmigration, little is known about the active role the endothelium itself plays during such processes. Our

063684) to JE and (DPI2015-64221-C2-1-R) to JMG-A, and the European Research Council (StG 306571) to JMG-A. EM is grateful for supports from the Cancer Research UK Multidisciplinary Award [C57744/A22057], CRUK-UCL Centre Award [C416/A25145] and Leverhulme Trust Research Project Grant (RPG-2018-443). EM was the recipient of the Wellcome Trust-Massachusetts Institute of Technology Fellowship (WT103883). The funders had no role in study design, data collection and analysis, decision to publish, or preparation of the manuscript.

Competing interests: The authors have declared that no competing interests exist.

computational model, together with new data, highlights the dynamic nature of endothelial cells, leading to gap formations through mechanical processes within the endothelium, without influence of cancer or immune cells. Thus, our results highlight the need to take the active mechanics of the endothelium into account when devising strategies to overcome the adverse effects of endothelial gap formation during inflammation or cancer.

Introduction

Immune and cancer cells alike are characterized by their ability to migrate within the vasculature and then to leave the vasculature into different tissues. These processes are crucial for a functioning immune system to fight acute infections [1] or participate in wound healing [2]. However, chronic inflammation or tumor metastases are ultimately also initiated by extravasating immune or cancer cells, respectively [3, 4, 5]. Hence, while extravasation is critical to cure communicable diseases, it is also a critical contributor to virtually all non-communicable disease, ranging from cancer to asthma, atherosclerosis, rheumatoid arthritis and heart diseases [6, 4, 7].

Much of the research on extravasation (often termed diapedesis in the context of immune cells) has focused on the role of the extravasating cell during this process, and how it interacts with the endothelial cells of the vasculature through which it is transmigrating. First, the extravasating cell needs to arrest in the vasculature. This may occur through single cells or clusters getting physically stuck in small capillaries, through the formation of adhesions, or both [8, 9, 10, 11, 12]. Such adhesion is mediated by molecules including P-and E-selectin, ICAM, VCAM or integrins [13]. The actual process of transmigration can occur through a single endothelial cell (transcellular extravasation) or, more commonly, in between two or more endothelial cells (paracellular extravasation) [14, 1].

During paracellular extravasation, it was investigated how the extravasating cell signals to the endothelial cells, leading to weakening of VE-cadherin-mediated cell-cell junctions and subsequently gap formation, through which the cells can transmigrate [8, 1]. Gap formation may, for instance, be stimulated by thrombin [15]. As such, molecular signaling events are firmly established as important contributors to extravasation of immune cells.

However, on a fundamental level, all the processes involved in extravasation are mechanical processes. Transmigration, like other forms of cell migration, involves the generation of mechanical forces through the actomyosin cytoskeleton [16]. Moreover, the mechanical properties of the endothelium provide passive mechanical resistance [16]. For instance, increased endothelial cell and junctional stiffness will reduce paracellular extravasation rates [17, 14]. Interestingly, recent research established that active mechanical properties of the endothelial cells are also critical during endothelial gap formation [18, 19, 20], and the rearrangements of cytoskeletal structures are associated with changes in barrier function. For instance, a rich actin cortex parallel to cell-cell borders is associated with stabilized VE-cadherin junctions and thus tight barriers [21, 22], whereas actomyosin stress fibers pulling radially on junctions can lead to junctional remodeling [18, 23]. Additionally, actin-rich pores can actively contract to prevent leakage during extravasation [24]. However, there is still a lack in mechanistic and systems level understanding of the different roles of active and passive mechanical properties of the endothelium.

Mathematical multiscale models are powerful tools to investigate the interplay of different physical drivers of biological processes. Many different approaches have been employed to model and understand the dynamics of epithelial monolayers. Agent based models, where

individual cells are explicitly taken into account, include center based models (CBM) [25], vertex models [26, 27] and deformable models (DFM) [28, 29]. However, these models do not explicitly model cell-cell adhesion dynamics in a way that leads to the experimentally observed gap formation in monolayers of endothelial cells, and can thus not easily be employed to study this problem so crucial for cancer and immune transmigration.

In this paper, we introduce a mathematical multiscale model of the mechanics of an endothelial monolayer where each endothelial cell contains contractile actin structures that may contract radially or in parallel to the plasma membrane. Then, cells are tethered to neighboring cells by cell-cell junctions that can dynamically form and break in a force-dependent manner. We employ this model to investigate the mechanisms of gap formation in an endothelial monolayer. Interestingly, we find that gaps open dynamically in the absence of any extravasating cells. These gaps form preferentially at the vertices where three or more endothelial cells meet, as opposed to the borders in between two cells. This is in line with our experimental data obtained in-vitro from quantifying gap formation of monolayers of human umbilical vein endothelial cells (HUVECs) seeded on glass. We quantify the frequency of gap openings as well as the duration of gap openings, obtaining good agreement between numerical predictions and experiments. Moreover, through multi-dimensional parameter studies, the mathematical model is able to give us insights into the physical and molecular drivers of the gap formation and gap dynamics. The model predicts that active and passive mechanical forces play an important role in the initial gap formation and in controlling size and lifetime of gaps once they initially formed. The catch bond nature of the cell-cell adhesion complexes as well as the force-dependent reinforcement of adhesion clusters may both stabilize junctions in response to forces acting on them. However, while the catch bonds ultimately weaken when forces are increased beyond the maximal lifetime of a single molecular bond, the force-dependent reinforcement will increase adhesion strength with increasing force [30, 18]. While the catch bond nature and the force dependence of the adhesion clustering processes both crucially influence gap opening frequencies, we find that gap lifetime and gap size are even more sensitive to the passive mechanical properties of the cell. Increased stiffness of the membrane/cortex and, even more notably, of the actin stress fibers will reduce lifetime and size, since the cells will then increasingly resist opening gaps through counteracting forces. On the other hand, we find that changes in bending stiffness of the membrane/cortex may have gap promoting or inhibiting effects.

Our model predictions of gap opening frequency and lifetime at both cell vertices and borders are validated by experiments observing such gaps in endothelial monolayers in the absence of any extravasating cell. The results thus challenge the paradigm that all extravasating cells primarily cause gap opening through interactions with the endothelium [1, 8, 31]. We then show experimentally that extravasating cancer cells indeed primarily extravasate at vertices, in line with similar observations for neutrophils [32]. Moreover, we show that cancer cells prefer to extravasate at vertices even when they initially attached to the endothelium at two-cell borders. This suggests that, even though extravasating cells can actively interact with the endothelium during transmigration, as shown in earlier studies, they may also take advantage of the autonomous occurrence of a gap, as predicted and verified to occur in our model. In summary, our work highlights the importance of taking the dynamic and autonomous mechanical properties of the endothelium into account when trying to understand gap formation and extravasation.

Computational model of endothelial monolayers

We present a novel model of an endothelial cell (EC) monolayer that incorporates different intracellular mechanical structures and dynamical cell-cell adhesions. The intracellular

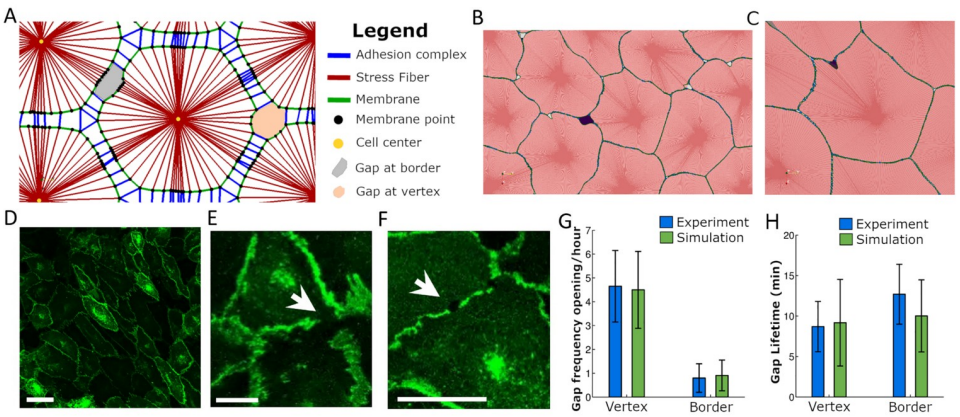

Fig 1. Endothelial gaps open preferentially at vertices. A: Main components of the model. Cells are formed by stress fibers (red), membrane segments (green) and membrane points (black). Membrane points are binding sites at which cell-cell adhesion complexes (blue) may connect to membrane points on adjacent cells and thus mechanically link these cells. When these adhesions break as a consequence of the force-dependent binding law, gaps in the endothelium are generated. Gaps can be generated at a two cell border (grey) or at a vertex between three or more cells (orange). B, C: Simulation of endothelial monolayer dynamics. Green denotes cell membrane and red the inside of a cell (darker red are the stress fibers that compose the cell). Dark purple denotes a detected gap. B: Gap at a vertex. C: Gap at border. D-F: Endothelial monolayer of HUVEC cells expressing VE-cadherin-GFP on glass. Gap opened at vertex (E) and border (F). Scale bars are 50μm (D) and 20μm (E,F), respectively. G, H: Quantification of gap opening frequency and gap lifetime at vertices or borders, respectively. Simulations correspond to the reference case. Error bars show the standard deviation.

https://doi.org/10.1371/journal.pcbi.1006395.g001

mechanical state is determined by radial contractile actin stress fibers and the cell membrane together with the actin cortex. For simplicity, we combined membrane and cortex into single viscoelastic elements, composed of an elastic spring and a viscous damper, that we refer to, from now on, as membrane elements. The radial stress fibers are also modeled by viscoelastic elements with different mechanical properties from the membrane, similar to a model of epithelial cells [28] (see Fig 1A). Neighboring cells may form cell-cell adhesions at adjacent nodes, and the resulting adhesion bond is modeled through a spring. The passive mechanical properties of the monolayer are thus modeled through a network of connected elastic and viscoelastic elements, similar to models of epithelial sheets [29, 28]. Since we are interested in studying the opening dynamics of gaps in the endothelial barrier, we explicitly simulate the dynamical binding of adhesion complexes. Contractions represent myosin motor activity that is known to exhibit randomness [33], so we employ Monte-Carlo simulations to estimate the occurrence of such forces as well as that of protrusive forces due to actin polymerization. The forces are then redistributed across the network of connected viscoelastic elements. Cell-cell adhesion complexes that mechanically link neighboring cells can dynamically bind and unbind in a force-dependent manner. The adhesion complexes in the model provide an effective description of both bonds of cell-cell adhesion molecules (such as VE-cadherin) and bonds of these adhesion molecules to the cytoskeleton. Cadherins and adhesion-cytoskeleton bonds are known to increase their binding strength in response to smaller forces, before they ultimately rupture [34]. This catch-bond type behavior is included in our model, and unbinding is thus simulated through a force-dependent Monte-Carlo simulation. Moreover, the number of VE-cadherins in an adhesion complex is modeled through a force-dependent adhesion clustering mechanism, as described in [18, 23, 35, 36, 37]. A more detailed description of the mathematical model and its numerical implementation is given in S1 Text.

We employ our endothelial monolayer model to explore the dynamics of endothelial cell junctions. We predict the frequency, size and duration of gaps, as well as the preferred

geometrical locations of the gap formation, and compare the predictions with our experimental measurements. The parameters used in the simulations are detailed in S1 Table. After comparing our predictions with the experimental results, we perform sensitivity analyses to investigate how cell mechanical properties, cell-cell adhesion characteristics and myosin generated forces regulate the formation, lifetime and size of gaps in the endothelium.

Summary of major model parameters

Here we present a summary of the major parameters of the model that had a significant impact on our model behavior, and were consequently thoroughly investigated through sensitivity analysis in the remainder of this paper. Table 1 lists all these parameters, and for a complete list and discussion see the Supporting Information. The main parameters investigated are related to cell mechanical properties, adhesion properties or myosin force generated processes.

Cell mechanical properties are dictated by stress fiber stiffness (K_{sf}), membrane stiffness (K_{memb}) and bending stiffness (incorporated through a rotational spring constant, K_{bend}). Stress fiber stiffness controls the rigidity of the interior of the cell, whereas membrane stiffness controls the rigidity of the membrane and the adjacent actin cortex. Bending stiffness acts on the membrane nodes depending on the relative orientation between the edges connecting at a given node.

Adhesion properties are controlled by the mechanical properties of the adhesion complexes and their binding and unbinding rates. Adhesion complex mechanics are modeled by linear springs, controlled by their stiffness constant, K^0_{adh}. The binding rate depends on distance and can be controlled by the adhesion complex density, ρ_{adh}. We then model the reinforcement of a bond that is already formed by the additional recruitment of adhesive proteins into the bond. Reinforcement is force dependent and can be controlled by the binding rate constant for adhesion reinforcement, k^0_{reinf}. Unbinding follows a catch bond behavior. The catch bond unbinding curve can be modified through two rate coefficients: k^0_s, which represents a slip bond, and k^0_c, which is the additional parameter characterizing the initial increase in the bond lifetime with force (see S12 Fig).

Then, the model includes contractile forces due to myosin motor activity, and protrusive forces that may arise due to actin polymerization. These forces can be directed radially (following the stress fibers direction) or in a tangential direction (following membrane segments). In the sensitivity analysis we have varied the magnitude of contraction forces in the radial direction (F_{Radial}) and in the tangential direction (F_{cortex}).

Table 1. List of parameters used in the sensitivity analysis.

Parameter	Symbol
Stress fiber stiffness	K_{sf}
Membrane stiffness	K_{memb}
Rotational spring constant	K_{bend}
Adhesion complex stiffness constant per bond	K^0_{adh}
Adhesion complex density	ρ_{adh}
Binding rate for adhesion reinforcement constant	k^0_{reinf}
Unbinding rate coefficient for catch curve	k^0_c
Unbinding rate coefficient for slip curve	k^0_s
Maximum force due to radial contraction	F_{Radial}
Maximum force due to cortical tension	F_{cortex}

https://doi.org/10.1371/journal.pcbi.1006395.t001

Results

Gaps open preferentially at vertices

Fig 1B and 1C and S1 Movie show typical simulations of the monolayer dynamics of the computational model. We observe that gaps open preferentially at vertices, i.e. the intersections of three or more cells, as opposed to the border between two cells. We have quantified this by counting the total number of gaps formed as well as their lifetime at borders and vertices of the cell in the center of the monolayer, and showed that our model predictions are in line with the experimental observations (Fig 1G and 1H). These experiments were performed by seeding HUVEC cells on glass, where they formed a continuous monolayer. The gaps were experimentally quantified through inspection of visible gaps within the VE-cadherin-GFP signal in the monolayer (arrows in Fig 1E and 1F). Controls simultaneously showing VE-cadherin-GFP and CD31 staining show that the VE-cadherin gaps are also visible in the CD31 staining, indicating that the VE-cadherin gaps correspond to real physical gaps between two or more cells S7 Fig (see Methods for further details of the experimental setup and quantification). Vertices are points where more than two cells exert forces and where tangential force components naturally propagate to. Therefore, it is expected that stress concentrates at the three cell vertex rather than at the two cells borders, and the simulations confirm this hypothesis (Supplementary S9 Fig and S3 Movie). The forces on adhesion clusters at the vertices are thus more likely to exceed the corresponding force of maximal lifetime of the bonds, as will be discussed in more detail below.

Mechanical properties of cell-cell adhesion complexes limit endothelial gap opening frequency

We study how variations in the mechanical properties of the cells, the cell-cell adhesion complexes or force variations affect the rate of gap formation. Fig 2A and 2B show how passive mechanical properties of the cell affect both the frequency (Fig 2A) and the location of the gap openings (Fig 2B). Increasing stiffness of either the membrane or the stress fibers provokes a decrement of the gap generation frequency (Fig 2A and S4 and S5 Movies). This is intuitive, since increasing stiffness stabilizes the movements of cells and makes the monolayer less dynamic. On the other hand, the location of the gap openings (i.e. whether they occur at a vertex or border) is critically affected by membrane stiffness at low values, until it stabilizes for intermediate and high membrane stiffness. In contrast, stress fiber stiffness affects gap location for very high stiffness, where gaps are almost fully prevented from opening at the borders (Fig 2B). Interestingly, increasing bending stiffness first increases gap generation up to a maximum point, before it leads to a decrease in gap opening frequency (Fig 2A). For small to intermediate bending stiffness, the frequency of gap openings increases, since bending stiffness is critical for effective force propagation between neighboring adhesion sites at vertices. When a single adhesion complex ruptures, bending stiffness leads to increased forces on neighboring adhesion complexes. After a peak in gap opening frequency at intermediate bending stiffness, a drop in the gap formation is observed for higher bending stiffness. This is caused by the resulting stabilization of the existing gaps at vertices. This high bending stiffness opposes sharp corners of the membrane at vertices and thus favors stable gaps that are permanently open, implying no new gaps are formed (S7 Movie). On the other hand, at cell borders, a high bending stiffness implies that if a single adhesion cluster is ruptured, the forces on it are redistributed across many neighboring adhesion sites and this stabilizes the borders (Fig 2B).

Turning to the role of cell-cell adhesion complex properties, our model shows that as the junctions become more stable, gaps open less frequently (Fig 2D). To increase cell-cell junction

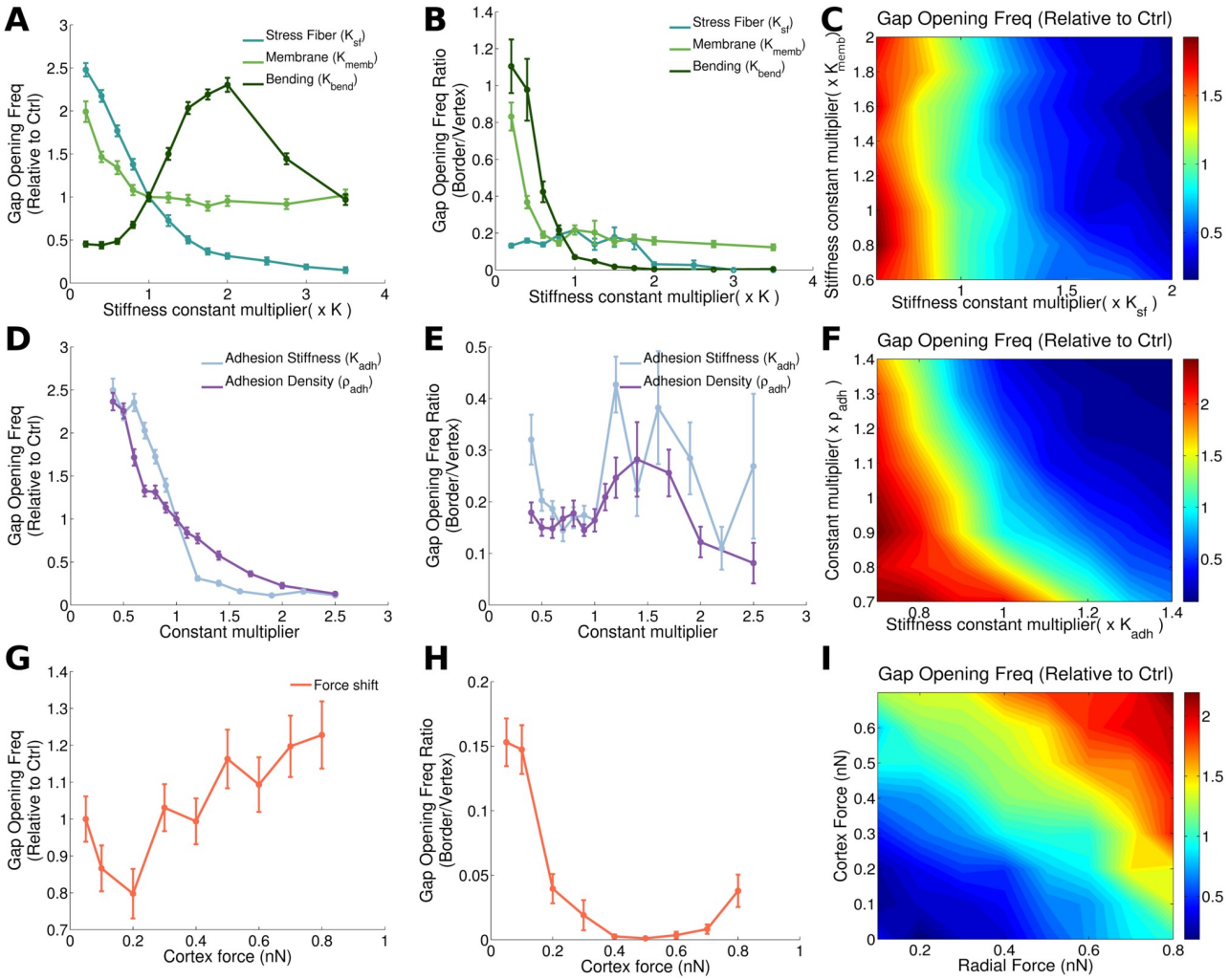

Fig 2. Intracellular and cell-cell junctional mechanical properties dictate gap opening dynamics. The first column (A, D, G) correspond to the total number of gaps (vertex plus border) generated per time, compared to the reference case (which, by definition, corresponds to the value 1 on the y-axis). The second column (B, E, H) shows the ratio of gaps that occur at a two cell border to the gaps that originate at a three cell vertex. Error bars show to the standard error. The third column (C, F, I) shows the impact of a two parameter variation in the gap opening frequency. The first row shows results from varying cell mechanical properties (stress fiber, membrane and bending stiffness (A, B)), and simultaneous variations of stress fiber and membrane stiffness (C). In the second row (C-F) properties of cell-cell junction are changed: adhesion stiffness and adhesion density. The third row shows results for increasing cortical force, keeping the total force constant (G and H) or varying both forces simultaneously (I).

https://doi.org/10.1371/journal.pcbi.1006395.g002

stability, we increase the mechanical stiffness of individual adhesion bonds, or the density of adhesion molecules. These results are in line with previous experimental work [14], which reported that more stable cell-cell junctions result in fewer transmigrating cells. While the total number of gaps at either vertex or border decreases with increasing cell-cell adhesion complex stiffness or cell-cell adhesion density available for binding, we see that there are no significant differences between gaps generated at the vertex and gaps generated at the borders (Fig 2E).

Fig 2G and 2H show the impact of changing the cortical and radial forces, where the total force is kept constant (when the radial force decreases, the cortical force is increased by the same magnitude). This is biologically relevant since cells are known to shift their cytoskeletal compartments in a context dependent manner [38]. In fact, cell monolayers subjected to shear flow have been reported to increase cortical actin while decreasing stress fibers [14].

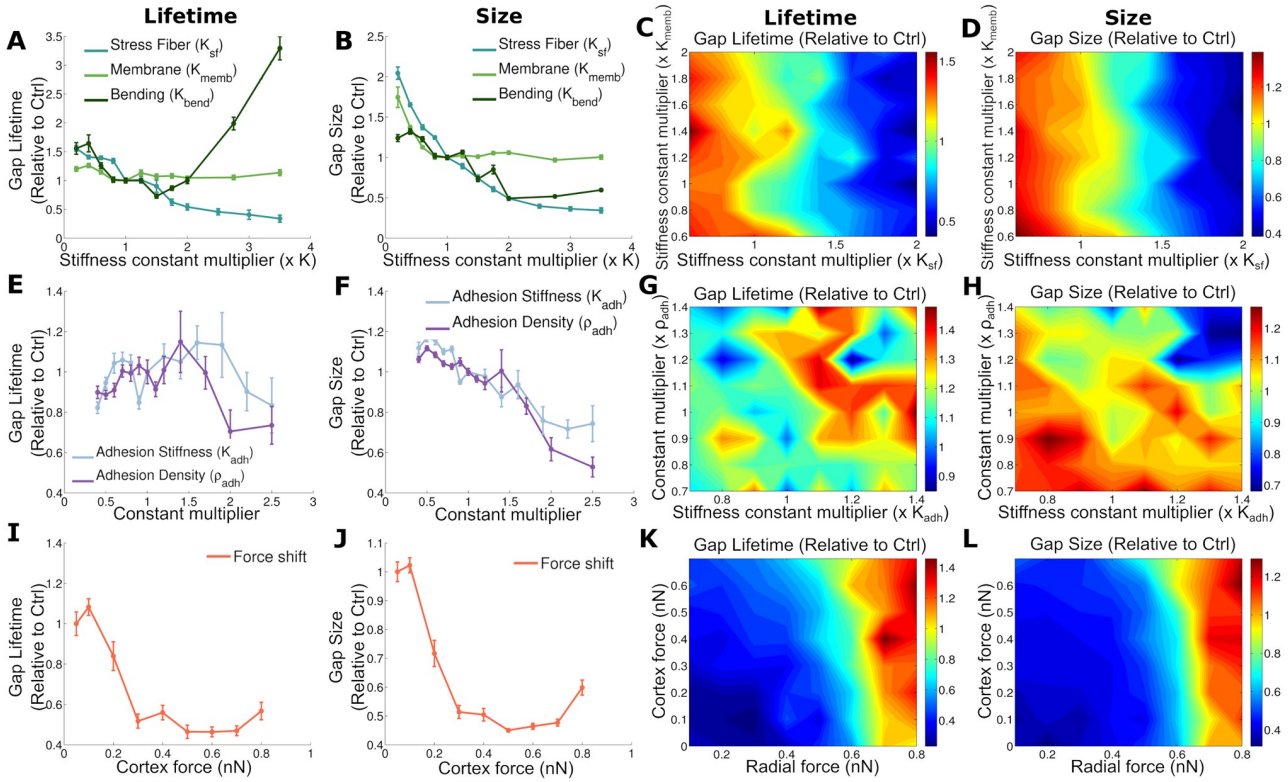

Fig 3. Impact of cell mechanics and cell-cell junctions properties on lifetime and size of gaps. Average lifetime of gaps ratio (divided by control case) in first column and average size in second column. Note that the point where the x and y axes values are 1 corresponds to the reference case. Error bars show to the standard error. A, B: Impact of membrane, stress fiber and bending stiffness. E, F: Impact of cadherin properties: stiffness and cadherin density (which affects the binding probability). I, J: Changing cortical force while keeping total force constant. Effect of two parameter variation on gap lifetime (third column) and size (fourth column). C, D: variation of membrane and stress fiber stiffness. G, H: Adhesion stiffness versus adhesion complex density variation. K, L; Cortical and radial force variation.

https://doi.org/10.1371/journal.pcbi.1006395.g003

Endothelial cells in particular, are known to exhibit both radial and tangential stress fibers with a different effect on gap opening dynamics [39]. As the force shifts from radial to cortical forces, total gap formation fluctuates with a slight increase as cortical forces increase (Fig 2G). For high cortical forces, the gaps also clearly tend to localize more at the vertices (Fig 2H). This is because contractions parallel to the membrane result in force concentrations at the vertices. For very high cortex forces, the typical stresses on adhesion clusters at the vertices may thus be higher than the force where the lifetime of catch bonds peaks (Supplementary S12 Fig), explaining the small increase in the number of gaps formed (Fig 2G). On the other hand, we will later show that these gaps formed at high cortical forces are typically small and have a short lifetime, limiting their potential for extravasation (see Fig 3I and 3J).

To take into account that molecular or physical perturbations may simultaneously affect multiple parameters, we now study how variations of pairs of these parameters at the same time may influence the monolayer integrity and the localization of the gap formation. Although, we have previously seen in Fig 2A that membrane and stress fiber stiffness have a similar effect on the gap opening frequency, in Fig 2C we can observe how the effect of varying stress fiber stiffness is clearly predominant over the effect of varying membrane stiffness. Fig 2F shows the impact of varying cell-cell adhesion stiffness and cell-cell adhesion complex density available for binding. Interestingly, there is a synergy between both parameters on regulating gap opening frequency, as evident through the curved shape of the levels of equal gap

opening frequency (Fig 2F). In Fig 2I we show the combined role of cortex and radial forces, thus not keeping total force fixed as in Fig 2G and 2H. This confirms that total force is the main driver of gap opening frequency, as opposed to a redistribution of forces between cortex and stress fibers (Fig 2I).

Passive cell-mechanical properties dictate endothelial gap lifetime and size

The lifetime and size of a gap are physical parameters that may also limit a cancer or immune cell's potential to extravasate through the monolayer. Here, we show how the lifetime and size of a gap are influenced by cell mechanical and junction properties, without the presence of extravasating cells (Fig 3). We observe that membrane stiffness has a marginal influence on the life time of the gap, whereas increasing stress fiber stiffness clearly reduces the time that a gap is open and the gap size (Fig 3A and 3B). Indeed, higher stress fiber stiffness will result in mechanical resistance to an opening gap and thus inhibit the propagation of the defect in the cell-cell junctions, leading to a stabilization of the monolayer (see S4 and S5 Movies). The dominance of stress fiber stiffness over membrane stiffness in regulating lifetime and size remains valid in a broad range of parameter values (Fig 3C and 3D).

Interestingly, increasing bending stiffness to high values may increase gap lifetime (Fig 3A). This is because higher bending stiffness will resist deviations from straight membranes. Thus, at straight borders, higher bending stiffness will resist gap openings whereas at vertices with high curvature, cells are more likely to adapt their shape resisting high curvature, thus favoring opened gaps. The dynamics of the monolayer for low bending stiffness is shown in S6 Movie.

Fig 3E and 3G show that adhesion complex stiffness and density at low values do not have a big impact on lifetime, however as they increase, lifetime starts to decrease. Both stiffness and density have a similar effect, since the total stiffness of an adhesion complex depends on both density and single bond stiffness (Eq. S10). Higher stiffness of the adhesion complex leads to more passive mechanical resistance to gap openings, and this effect dominates for high stiffness. The level of noise due to repeats of our MC simulations is higher for these adhesion parameters than for the parameters determining cell mechanics. Likewise, for the gap size, the stabilizing effect of both adhesion complex stiffness and density dominates and leads to a reduction in gap size (Fig 3F and 3H). However, the effect of increasing the density is slightly stronger than that of increasing single bond stiffness. This is because the density affects not only adhesion complex stiffness (Eq. S10), but also the rate of forming new adhesion complexes (Eq. S9) and the rate of reinforcing existing bonds (Eq. S11). These effects together thus synergize to stabilize gaps and prevent them from growing too large.

Earlier, we have shown that a shift in the force (from radial to cortical) produces an increment in gap formation (Fig 2G). Fig 3I and 3J show that this shift in the force reduces gap lifetime and size. This indicates that, although the frequency of opening is increased, these gaps are smaller and last shorter in time which may reduce paracellular extravasation, as suggested in previous experimental work [14]. Combined changes of cortical and radial force show that although both kinds of forces are needed to increases gap size and lifetime, the impact of radial forces is clearly predominant over the impact of cortex forces (Fig 3K and 3L). This is intuitive, since radial forces clearly separate cell borders generating bigger gaps and make them harder to close, whereas cortical forces distribute forces to vertex regions. This does not provoke large cell deformations, which is reflected in the low impact on the gap size and lifetime observed.

Catch bonds facilitate regimes of maximal endothelial stability

In Fig 4A–4C we show the impact of varying the catch-bond unbinding parameter k_c^0 that shifts the location of the peak of maximal lifetime of a single catch bond, while we maintain

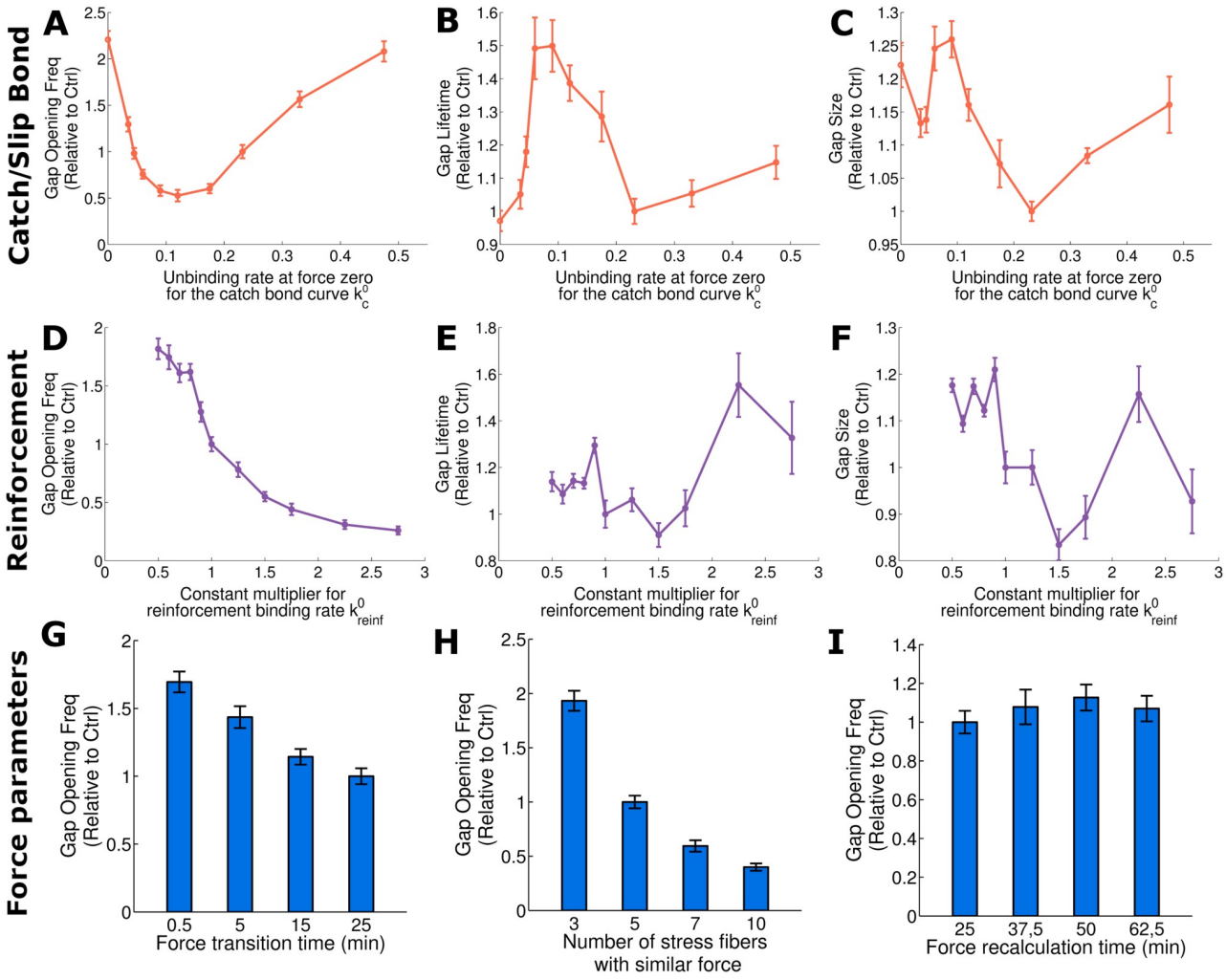

Fig 4. Effect of the maximal lifetime of a catch bond, the cadherin reinforcement and the force application on the gap opening dynamics. First row (A-C) shows the impact of shifting from a pure slip bond ($k_c^0 = 0$) to a catch bond. As k_c^0 increases, the peak of stability moves to higher force while we fix the magnitude of a single bond lifetime. Second row (D-F) shows reinforcement analysis varying k_{reinf}^0. Results are normalized with reference case values and are shown for gap opening frequency (A, D), gap lifetime (B, E) and gap size (C, F). Third row shows the effect of force application on total gap opening frequency. G: Total gap opening frequency depending on the time that takes to make the force transition. Longer time means smoother force changes. H: Total gap opening frequency depending on the number of stress fibers at which the same force is distributed. I: Variation in force recalculation time for all types of forces considered in the model. Note that the reference case corresponds to the point where y and x axes values are 1 in figs A to F. Error bars show the standard error.

https://doi.org/10.1371/journal.pcbi.1006395.g004

the actual maximum value through simultaneously shifting the slip-bond unbinding parameter k_s^0 (Eq. S12 and S12 Fig). We observe that for a pure slip bond (corresponding to $k_c^0 = 0$), gaps occur at a higher rates than for small nonzero values of k_c^0. Increasing k_c^0 further leads to a minimum in gap opening frequency, from which the frequency increases again. This minimum corresponds to a maximum of stability, where forces on the adhesion complexes are similar in magnitude to the peak of stability of the catch bond. Consequently, shifting the location of that peak even further towards higher forces (by increasing k_c^0 even further) means we destabilize the catch bonds again. Note that the gap lifetime and size of gaps are much less influenced by the location of the catch bond maximum than the gap opening frequency.

In Supplementary S11 Fig, we show histograms of the forces on adhesions comparing the number of bound clutches, the number of unbinding events, and the ratio of unbound to total

bonds for slip bonds ($k_c^0 = 0$) to the catch bond with reference values ($k_c^0 = 0.27s^{-1}$). We see that adhesions in the catch bond case bear and disengage at higher forces than for the slip bond case, confirming that the typical forces on bonds are of such magnitude that the catch bond nature stabilizes the junctions.

In Fig 4D–4F we modify the reinforcement binding rate k_{reinf}^0 to check the influence of the reinforcement. This is different from the previous analysis where the adhesion complex density available for binding was changed, since now the binding probability based on distance is not affected (Eq. S9). However, we see the same trend of increasing stability with increasing k_{reinf}^0 (Fig 4D), in line with the result obtained from varying cadherin density (Fig 2D), suggesting that binding is mainly regulated by this reinforcement process. Similar to the catch bond, we see that adhesion reinforcement is less important in determining gap size or lifetime (Fig 4E and 4F) than in regulating gap opening frequency.

Force fluctuations and distribution regulate gap opening dynamics

We have shown that both the magnitude of forces and the cytoskeletal compartment that generates the forces (stress fibers or cortex) affect gap opening frequency, size and and lifetime. Besides these broad compartments, many other biological and physical parameters affect how forces ultimately act on cell-cell junctions: Forces may act in a directed manner due to larger parallel actin bundles and synchronous myosin activation, e.g. initiated through waves of activators [15], or may act more randomly [33]. We test variations in force applications through parameters that affect the transition time when forces change ($t_{Transition}^{Force}$), through spatial force distributions and through the velocity at which forces are modified. In Fig 4G we observe how increasing the force transition time $t_{Transition}^{Force}$ slowly reduces the gap opening. This is due to the fact that a slower, persistent application of forces leads to a redistribution of the forces through rearrangement and remodeling of the cell. It is consistent with experimental works that showed that force fluctuations influence gap opening dynamics [15].

Then, distributing the same radial forces over several adjacent stress fibers reduces gap opening frequency (Fig 4H). More spatially distributed forces are less capable of damaging cell-cell junctions than localized peak forces, since such high peak forces are required to overcome the catch bond maximal lifetime. Likewise, high peak forces lead to longer lifetime and larger size of the resulting gaps (Supplementary S13C and S13D Fig).

Next we observe the effect of force persistence in time. We vary the force recalculation time parameter (equally for all forces) in Fig 4I. Results show that the time that forces are applied does not have a big influence on gap formation. This suggests that cells are able to adapt to forces in longer time scales and therefore it is not the time that forces are applied what regulates gap formation, but the transitions of force fluctuations and their spatial distribution.

Cancer extravasation mimics autonomously occurring endothelial gap dynamics

To demonstrate that the geometry of the gap opening dynamics is physiologically relevant, we quantified the characteristics of extravasating cancer cells through monolayers of HUVECs, as shown in S9 Movie. Here, a tumor cell is seen transmigrating through an endothelial monolayer at a tricellular junction as delineated by VE-cadherin GFP, followed by gap-closure after the tumor cell has completely cleared the barrier. Fig 5A shows the ratio of tumor cells that extravasated at vertices, relative to borders. We see that tumor cells preferentially extravasate at the vertices, in line with the previously observed increased frequency of gaps opening there (Fig 1G) and similar observations of extravasating neutrophils [32]. Moreover, even if cancer

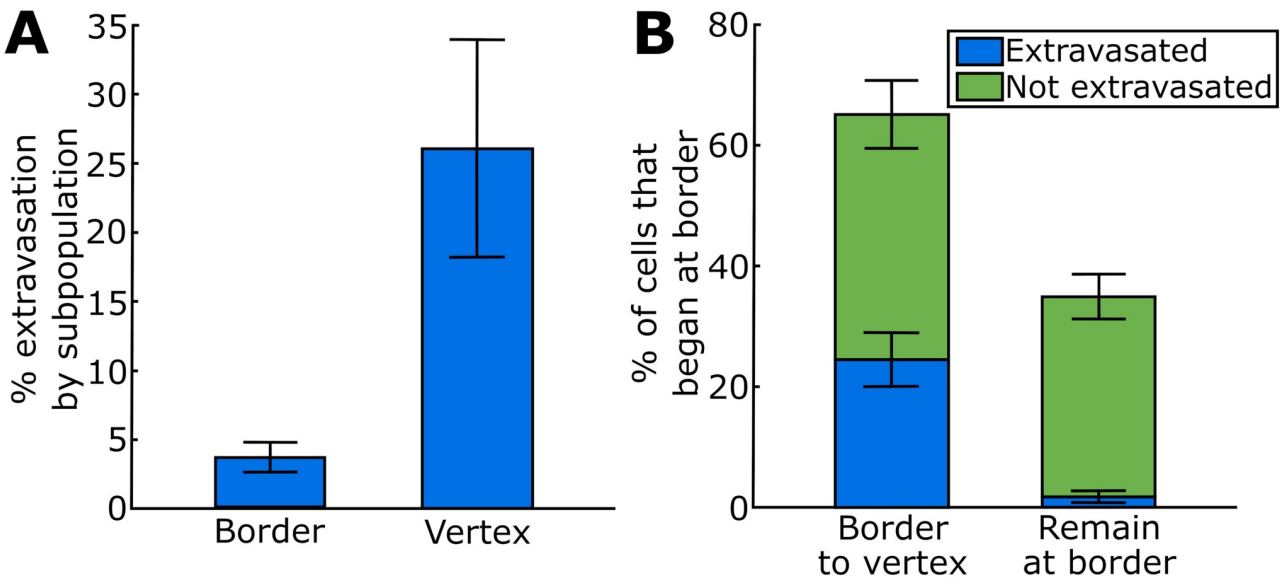

Fig 5. Cancer cells preferentially extravasate at vertices, even when they first attached to endothelial cell borders. A: Extravasation of cancer cells in dependence of the location where they transmigrate. B: Extravasation of cancer cells that initially attached to endothelial cell borders, in dependence on whether they extravasate or not and on where they extravasate. Error bars show the standard deviation obtained from 6 (in A) or 4 (in B) repeats of each experiment, performed in separate devices, where in each device about 100-150 extravasating cells were imaged.

https://doi.org/10.1371/journal.pcbi.1006395.g005

cells initially arrest at the border between two endothelial cells, they are much more likely to extravasate at a vertex at later points in time, rather than at the border where they initially attached to, perhaps first through migration on the surface of the endothelium and subsequent preferential attachment to points of exposed basement membrane as a result of inherent EC junctional dynamics (Fig 5B). This could suggest that in addition to the possibility of cancer cells actively signaling to open gaps in the endothelium, endothelial barrier dynamics itself can also present the cancer cells with opportunities to begin the transmigration process.

Discussion

The computational model presented in this paper allowed us to study how gaps in an endothelial monolayer initially open, grow, stabilize and finally close, and we identified which physical properties dominantly regulate each stage.

The model simulates a cell monolayer in two dimensions. Adhesion between cells is simulated through binding or unbinding of adhesion complexes located on adjacent cells. These adhesion complexes are dynamically engaging and disengaging as the myosin generated forces cause cell deformations. Because of cell-cell adhesion rupture, gaps between the cells are formed. To perform our simulations, the model is based on a number of assumptions that simplified the model. First of all, due to the typically small height (about $3\mu m$) of endothelial cells [40], we neglected the third dimension perpendicular to the monolayer. However, disruptions of the spatio-temporal dynamics of adhesion molecules and cytoskeletal organization in the third dimensions are likely to impact gap formation. Incorporating such effects into our model would consequently require a 3D model of a cell with more detailed descriptions of the subcellular mechanics. However, the purpose of our model was to demonstrate the broad impact of subcellular mechanical structures on gap formation. For this reason, we modeled the cells in two dimensions and included only radial stress fibers and contractile actin fibers parallel to the membrane. This was motivated by experiments that indicated different roles of these actin

structures on gap formation [23]. Each discrete adhesion complex is simulated as one cluster to simulate recruitment of proteins such as vinculin or talin, without increasing the total number of components in the simulation. Myosin generated forces included in the model are assumed to occur only in the direction of the stress fibers or membrane.

Supplementary S14 Fig summarizes some of our key conclusions: By comparing our reference case with extreme variations of very low stress fiber or membrane stiffness, we see that both passive mechanical properties and adhesion complex properties are important in controlling gap opening frequency (Supplementary S14A Fig). On the other hand, the lifetime and especially size of gaps increases significantly with lower stress fiber or membrane stiffness, since the softer cells are more likely to deform and adapt in response to the opened gap (Supplementary S14B and S14C Fig). We also verify that stress fiber stiffness influence is stronger than membrane stiffness influence. In contrast, properties of the cell-cell adhesions strongly affect the frequency of the gap openings, but less so their lifetime or size. Indeed, decreasing the density of adhesion bonds or the adhesion stiffness strongly increase the frequency of forming gaps (Supplementary S14A Fig), while only marginally affecting the size or lifetime of the gaps (Supplementary S14B and S14C Fig). These data thus summarizes our biological model where adhesion properties control the initial formation of gaps, while cell mechanical properties are critical in limiting the size and duration of opened gaps.

Our results that gaps open more frequently at vertices than at borders were true over wide ranges of parameters (Fig 2B, 2E and 2H). Only extremely small bending stiffness led to similar frequencies of gaps at vertices and at borders (Fig 2B). These results also show that earlier experimental observations, where neutrophils were found to extravasate preferentially at endothelial cell vertices, [32], can be explained through the mechanical dynamics of the endothelial monolayer alone. Consequently, this may be a general mechanism for extravasating cells, and we found a similar behavior with extravasating cancer cells (Fig 5). This finding is complementary to the extensive literature that suggests that chemical or mechanical signaling of extravasating immune or cancer cells to the endothelium facilitates extravasation [1, 8, 31]. There are many potential hypotheses why both the autonomous dynamics of the endothelial monolayer and the bidirectional signaling with the extravasating cells may play a role during extravasation: It may be that initial autonomously forming gaps are important for extravasating cells to sense a gap and they consequently signal to widen the gap or to keep it open. The gap sizes that the model predicts are of the order of magnitude of a few microns, which is enough for extravasating cells to protrude through the gap. Our previous study indicates that tumor cells can squeeze significantly when transmigrating through artificial gaps [16], so the autonomous gaps may be of sufficient size for complete transmigration. Nevertheless, endothelial gaps may widen during transmigration, so crosstalk between the transmigrating cell and the endothelium likely remains an important factor contributing to the likelihood and speed of extravasation. Then, whether bidirectional signaling or autonomous gap formation dominates the process may be cell type specific. For instance, it is still a major research question why certain cancer cells preferentially metastasize to certain organs [41]. We may speculate that not only the signaling of the specific primary tumor cells with an organ-specific type of endothelial cells influences the likelihood of extravasation [8]. Also, the mechanical properties of the endothelium of the target organs will likely play a major role. Our flexible modeling framework was tested with a HUVECs monolayer, yet, by changing the physical parameters of the model, it may be quickly adapted to other endothelia.

Besides testing our model with different endothelial cells, some other important steps towards validating our model conclusions in vivo will be to test our model with more realistic three dimensional microvasculature with blood flow, embedded in extracellular matrix and surrounded by supporting cells such as pericytes, fibroblasts or, for brain, astrocytes [41, 1].

Such real, in vivo microvasculature consists of vessels that are curved and exposed to shear stresses due to the flow. That, in turn, may be affected by extravasating cells that may obstruct blood flow. Similarly, matrix stiffness was shown to affect endothelial monolayer integrity [42, 43]. Some complications in validating our results in vivo involve the lack of available in vitro cultures that are required to provide high throughput, microscopy resolution and level of experimental control that is lacking in vivo, making direct comparison of computational models to in vivo experiments unfeasible. However, the recent rapid progress in developing more complex and organ specific in vitro assays of 3D microvasculature will make such validations feasible in the near future [44, 45, 46].

Our model is based on a number of simplifications. We do not consider the effect of extracellular matrix and substrate stiffness properties on monolayer integrity, despite the known effect of these properties on cell mechanics. It is important to remark that cells on glass may behave very differently than in vivo endothelial vessels. Our model also does not include the effect of fluid pressure or tangential stress due to fluid flow. Pressure and blood flow would induce additional forces over the monolayer that could affect gap generation processes. For example, it was observed [14] that tangential flow could induce the strengthening of cell-cell junctions, therefore reducing paracellular extravasation.

Modeling such complex environments presents a great challenge to both in vitro and in silico models. It is therefore essential to justify assumptions that can reduce this complexity and make the model development feasible. Here, we have assumed that the mechanics of the inside of a cell is determined by a fixed number of stress fibers, although it is known that inside the cell there are different polymer structures such as microtubules and intermediate filaments. Moreover, actin filaments are not fixed in time but appear and disappear depending on their stability and polymerization rates. To simulate all of this with high accuracy would require a completely different model in which the computational cost that would exceed current capabilities. For the purpose of this project, we focused on incorporating essential cell mechanical structures that have been implicated in the regulation of gap formation, and modeled a fixed number of stress fiber similar to other works [28, 29]. Similarly, we have simulated adhesion complexes as discrete elements that can bind two membrane points of neighboring cells. In real cells, adhesion complexes between cells are formed by a great variety of proteins such as VE-cadherins, α-catenin, talin or vinculin. While the spatio-temporal dynamics of each of these adhesion molecules likely influences gap formation, no computational model can currently explain their precise organization in adhesion complexes and their resulting effect on gap formation. Consequently, our model included an effective term that describes the force dependent recruitment of adhesions, as observed in different experimental studies [23, 20].

Moreover, there are also challenges to the mathematical modeling of complex 3D microvasculature. Modeling of epithelial sheets in 3D has proved challenging, with some recent interesting progress after decades of mainly focusing on epithelial monolayers in 2D [47, 48, 49]. These models are based on frameworks such as vertex models, where the dynamics of each cell is incorporated into the dynamics of vertices between cells. There are many other modeling frameworks that can capture different aspects of the complex cell behavior, such as cell based models [50], immersed boundary models [51] or subcellular element models [52, 53]. These modeling frameworks are, however, not directly suitable to predict the formation of gaps at either vertices or borders. Given these challenges, is was paramount to establish a 2D mathematical model of an endothelial monolayer that was validated with novel experiments and that was able to lead to insights into the mechanisms of endothelial gap formation.

Methods

Generation of HUVEC monolayers and image acquisition

Human umbilical chord vein cells (HUVECs) were transduced with VE-cadherin-GFP using methods described previously [45]. HUVECs at P7-10 were seeded onto 35 mm glass bottom Mattek dishes (at 3×10^5 cells/dish), which had been plasma treated for 30 seconds previously. Cells were allowed to grow to confluence (beyond 100%) in EGM-2MV (Lonza) for 3 days before imaging. Dishes were imaged on an Olympus FV1000 confocal microscope with magnifications of 30X (oil immersion), under an environmental chamber set at 37C and 5% CO2. The chamber was equilibrated for $\sim$ 30 min prior to the start of image acquisition. For time-lapse videos of junctional dynamics, z-stacks of $40\mu m$ ($4\mu m$ steps) were taken at intervals of 3 minutes.

Analysis of junctional disruption dynamics

Time-lapse images were appended and analyzed manually on ImageJ. A single unique junctional disruption is defined as a vertex or border with an observed gap of greater or equal than $3\mu m$, and are preceded and proceeded at some point in time with a closure (no visible gap in fluorescence greater than $0.6\mu m$). The number of junctional disruption events was counted for each border and vertex of an image over a total time period of 2 hours. Vertices and borders belonging to the same cells were still considered to be unique.

Analysis of tumor cell extravasation

Tumor cells were suspended in EGM-2MV (Lonza) and a concentration of 15,000 cells/mL, and 1mL of the suspension was gently added to each HUVEC monolayer. Cells were allowed to settle first for $\sim$10 minutes before acquisition of $t = 0$ images. For quantification of extravasation, z-stacks were taken at $3\mu m$ steps at an endpoint of 6 hours to image the entirety of the tumor cell and endothelial monolayer. Any tumor cell that has breached the endothelial layer as evidenced by protrusion extension across and beneath the endothelial layer was considered as "extravasated". Delineation of the endothelial barrier is visualized via CD31 staining (Biolegend, Cat # 303103) for 30 min in EGM-2MV at 37C and 5% CO2 prior to imaging.

Supporting information

S1 Text. Detailed description of the mathematical model.
(PDF)

S1 Table. Reference model parameters used in the simulation.
(PDF)

S1 Fig. Mechanical model of a single cell. The cell is presented in an initially hexagonal form, divided into a discrete number of membrane points. Physically, our membrane elements connecting the nodes represent the combined lipid bilayer with the actin cortex. Moreover, the nodes are connected to the center by stress fiber structure. Both of them are described by Kelvin-Voigt models with a contractile/protrusive element, but both have different parameters.
(TIF)

S2 Fig. Contribution of different passive intracellular forces. (A) Force due to stress fiber deformations. (B) Force due to membrane in-plane deformation. (C) Force due to membrane bending stiffness. (D) Force due to repulsion between membrane points of different cells.
(TIF)

S3 Fig. Cell generated forces. (A) and (B) Correspond to myosin forces: Radial force and Cortex force respectively. (C) Protrusive forces.
(TIF)

S4 Fig. Stress fiber remodeling. Due to myosin contractility, a change in the rest length of the stress fiber occurs accordingly to Eq. S15. This change in rest length is compensated by all the stress fibers in a proportional way. Note that only the rest lengths and not the current length of a stress fiber is modified.
(TIF)

S5 Fig. Model of the endothelial monolayer. A: Cells with a hexagonal shape are in a rest state and fully bound to their neighboring cells. Cell membrane (green), stress fibers (red), cadherin complexes (blue), membrane points (black). B: Boundary conditions: Points in the boundary of the monolayer (red) are fixed. In blue are membrane points and the cell centers.
(TIF)

S6 Fig. Paracellular gap. A gap (grey area) is delimited by the cell membrane (green) and the adhesion bonds binding the cells (blue). Red: cell stress fibers. Black dots: Membrane points.
(TIF)

S7 Fig. Gaps in VE-cadherin correspond to gaps in CD31. Endothelial monolayer stained with VE-cadherin (green, A) and CD31 (red, B). C: Merged image confirms that gaps observed within the VE-cadherin mediated cell-cell adhesions are also present within CD31, indicating that gaps seen in VE-cadherin are real physical gaps between the cells. Scale bar 100μm.
(TIF)

S8 Fig. Gap sizes predicted from simulations with reference parameters. Average size of the gaps generated at the vertices and borders. Parameters are the reference values as in S1 Table and error bars correspond to standard deviation of sample = 30.
(TIF)

S9 Fig. Stresses on the cell-cell adhesions. Homogeneous contractions are applied to all the hexagonal cells in the monolayer. Stresses concentrate on the adhesions at vertices, as opposed to the adhesions at border.
(TIF)

S10 Fig. Effect of two parameter variation on gap opening location. Shown is the ratio of gaps that occur at a two cell border divided by the gaps that originate at a three cell vertex. A shows results varying membrane and stress fiber stiffness. B shows properties of cell-cell junction are changed: cadherin stiffness versus cadherin density (binding rate). C shows results for varying cortical and radial force.
(TIF)

S11 Fig. Forces on bonds, comparing a pure slip bond and the catch bond law used as reference in the paper. First row (A, B) shows force histogram of cadherins that are bound for slip and catch bond respectively. Second row (C, D) cadherins force at which cadherins unbind for slip and catch bond respectively. Third row (E, F) shows the ratio obtained by dividing unbound cadheins by the sum of unbound cadherins and bound cadherins ($ub/(ub + b)$, where ub and b corresponds to unbound and bound cadherins respectively).
(TIF)

S12 Fig. Shift of force of maximal catch bond lifetime. Lifetime average for the bond in dependence on the force for different unbinding laws. Legend shows the parameter variation

to obtain the different curves.
(TIF)

S13 Fig. Effect of force application on gap size and lifetime. Corresponds to Fig 4. Left column corresponds to lifetime and right column to size. (A, B): Changes in the transition time of the application of the recalculated forces. Longer time means smoother force changes. (C, D) Variation in the number of stress fibers over which the same force is distributed. (E, F) Variation in force fluctuation time for all types of forces considered in the model. Error bars show to the standard error.
(TIF)

S14 Fig. Interplay of adhesion and cell mechanical properties controls different aspects of gap opening dynamics. Error bars show to the standard error. All parameters have been reduced one order of magnitude ($x10^{-1}$). (A) Gap opening frequency. (B) Average lifetime of the gaps. (C) Average size of the gaps.
(TIF)

S15 Fig. Time step analysis. The gap opening frequency depends on the time step used in our numerical simulations. Note that the time step multiplier is relative to the reference case (multiplier = 1). Error bars are the standard error. The results confirm that the time step selected for the reference case is low enough to ensure convergence of the results.
(TIF)

S16 Fig. Effect of the viscosities and the remodeling rate on the gap opening dynamics. Gap opening frequency, average lifetime and size in each column. Note that the point where x and y coordinates are 1 corresponds to the reference case. Error bars represent standard error. In the first row (A, B, C), results for medium and dashpot viscosities of the stress fibers and membrane and varied. Increasing viscosity reduces node movement, stabilizing monolayer dynamics. Medium viscosity has a higher effect on gap opening dynamics since it affects the overall timescale of all mechanical parts of the model. The stress fiber dashpot strongly influences gap lifetime and size; this is similar to the dominating effect of stress fiber stiffness over membrane stiffness on gap lifetime and size (Fig 3A and 3B). The second row (D, E, F) shows the effect of varying the constant for remodeling rate. Increasing the remodeling rate implies that cells are able to adapt their permanent shapes faster in response to deformations. Therefore, the frequency of gap openings increases with the remodeling rate (D). The gap lifetime and size broadly also increase, but less strongly then the opening frequency.
(TIF)

S1 Movie. Simulation of the endothelial monolayer dynamics. Gaps are more likely to appear in the vertex of three cells than at a two cell border. Green denotes the cell membrane, red the inside of a cell, with darker red being the stress fibers. Parameters are the reference values as in S1 Table.
(MP4)

S2 Movie. Experimental observation of an endothelial monolayer dynamics. Dynamics of a monolayer of HUVEC cells, corresponding to Fig 1D–1F.
(MOV)

S3 Movie. Stresses on the cell-cell adhesions. Homogeneous contractions are applied to a hexagonal cell, showing that stresses naturally concentrate on the adhesions at vertices, as opposed to the adhesions at the border. This leads to a faster gap generation at these areas.
(MP4)

S4 Movie. Altered monolayer dynamics due to low stiffness in the stress fibers. Not only gap opening frequency is increased under these conditions but also, gaps are critically larger compared to the reference case.
(MP4)

S5 Movie. Altered monolayer dynamics due to high stiffness in the stress fibers. Gap opening frequency is strongly suppressed for very stiff stress fibers.
(MP4)

S6 Movie. Altered monolayer dynamics due to low bending stiffness. Membranes can easily deform when forces are applied, reducing gap formation.
(MP4)

S7 Movie. Altered monolayer dynamics due to high bending stiffness. Cells tend to be more rounded, provoking a concentration of stress at the adhesions at the vertices and leading to gap generation in these zones. Gaps are bigger and difficult to close.
(MP4)

S8 Movie. Altered monolayer dynamics due to slip bonds. Gap opening frequency is clearly increased under these conditions compared to the reference case (based on catch bonds).
(MP4)

S9 Movie. Cancer cell extravasation occurring at endothelial cell vertex. MDA-MB-231 tdTomato (red) extravasating through a HUVEC endothelial monolayer at a vertex. Endothelial junctions are visualized via VE-cadherin GFP (green). After successful transmigration, cancer cells spreads and migrates below the monolayer, followed by the re-sealing of the endothelial gap. Images are taken every 12 minutes.
(MOV)

Author Contributions

Conceptualization: Michelle B. Chen, Roger D. Kamm, Fabian Spill.

Data curation: Jorge Escribano, Michelle B. Chen, Emad Moeendarbary.

Formal analysis: Jorge Escribano, Fabian Spill.

Funding acquisition: Jose Manuel Garcia-Aznar, Roger D. Kamm.

Investigation: Jorge Escribano, Michelle B. Chen, Fabian Spill.

Methodology: Jorge Escribano, Xuan Cao, Vivek Shenoy, Jose Manuel Garcia-Aznar, Roger D. Kamm, Fabian Spill.

Project administration: Jose Manuel Garcia-Aznar, Roger D. Kamm, Fabian Spill.

Resources: Jose Manuel Garcia-Aznar, Roger D. Kamm.

Software: Jorge Escribano.

Supervision: Jose Manuel Garcia-Aznar, Roger D. Kamm, Fabian Spill.

Validation: Emad Moeendarbary.

Visualization: Jorge Escribano.

Writing – original draft: Jorge Escribano, Fabian Spill.

Writing – review & editing: Jorge Escribano, Michelle B. Chen, Emad Moeendarbary, Xuan Cao, Vivek Shenoy, Jose Manuel Garcia-Aznar, Roger D. Kamm, Fabian Spill.

References

1. Vestweber D. How leukocytes cross the vascular endothelium. Nature Reviews Immunology. 2015; 15 (11):692–704. https://doi.org/10.1038/nri3908 PMID: 26471775
2. Park JE, Barbul A. Understanding the role of immune regulation in wound healing. The American Journal of Surgery. 2004; 187(5, Supplement 1):S11–S16. https://doi.org/10.1016/S0002-9610(03)00296-4.
3. Grivennikov SI, Greten FR, Karin M. Immunity, inflammation, and cancer. Cell. 2010; 140(6):883–899. https://doi.org/10.1016/j.cell.2010.01.025 PMID: 20303878
4. Murray PJ, Wynn TA. Protective and pathogenic functions of macrophage subsets. Nature reviews immunology. 2011; 11(11):723–737. https://doi.org/10.1038/nri3073 PMID: 21997792
5. Muller WA. How endothelial cells regulate transmigration of leukocytes in the inflammatory response. The American journal of pathology. 2014; 184(4):886–896. https://doi.org/10.1016/j.ajpath.2013.12.033 PMID: 24655376
6. Libby P, Okamoto Y, Rocha VZ, Folco E. Inflammation in atherosclerosis. Circulation journal. 2010; 74(2):213–220. https://doi.org/10.1253/circj.CJ-09-0706 PMID: 20065609
7. Mullin JM, Agostino N, Rendon-Huerta E, Thornton JJ. Keynote review: epithelial and endothelial barriers in human disease. Drug discovery today. 2005; 10(6):395–408. https://doi.org/10.1016/S1359-6446(05)03379-9 PMID: 15808819
8. Reymond N, D'Água BB, Ridley AJ. Crossing the endothelial barrier during metastasis. Nature Reviews Cancer. 2013; 13(12):858–870. https://doi.org/10.1038/nrc3628 PMID: 24263189
9. Luster AD, Alon R, von Andrian UH. Immune cell migration in inflammation: present and future therapeutic targets. Nature immunology. 2005; 6(12):1182. https://doi.org/10.1038/ni1275 PMID: 16369557
10. Kienast Y, Von Baumgarten L, Fuhrmann M, Klinkert WE, Goldbrunner R, Herms J, et al. Real-time imaging reveals the single steps of brain metastasis formation. Nature medicine. 2010; 16(1):116. https://doi.org/10.1038/nm.2072 PMID: 20023634
11. Wirtz D, Konstantopoulos K, Searson PC. The physics of cancer: the role of physical interactions and mechanical forces in metastasis. Nature Reviews Cancer. 2011; 11(7):512. https://doi.org/10.1038/nrc3080 PMID: 21701513
12. Follain G, Osmani N, Azevedo AS, Allio G, Mercier L, Karreman MA, et al. Hemodynamic Forces Tune the Arrest, Adhesion, and Extravasation of Circulating Tumor Cells. Developmental Cell. 2018; 45 (1):33–52.e12. https://doi.org/10.1016/j.devcel.2018.02.015. PMID: 29634935
13. Allingham MJ, van Buul JD, Burridge K. ICAM-1-Mediated, Src- and Pyk2-Dependent Vascular Endothelial Cadherin Tyrosine Phosphorylation Is Required for Leukocyte Transendothelial Migration. The Journal of Immunology. 2007; 179(6):4053–4064. https://doi.org/10.4049/jimmunol.179.6.4053 PMID: 17785844
14. Martinelli R, Zeiger AS, Whitfield M, Sciuto TE, Dvorak A, Van Vliet KJ, et al. Probing the biomechanical contribution of the endothelium to lymphocyte migration: diapedesis by the path of least resistance. J Cell Sci. 2014; 127(17):3720–3734. https://doi.org/10.1242/jcs.148619 PMID: 25002404
15. Valent ET, van Nieuw Amerongen GP, van Hinsbergh VWM, Hordijk PL. Traction force dynamics predict gap formation in activated endothelium. Experimental Cell Research. 2016; 347(1):161–170. https://doi.org/10.1016/j.yexcr.2016.07.029 PMID: 27498166
16. Cao X, Moeendarbary E, Isermann P, Davidson PM, Wang X, Chen MB, et al. A Chemomechanical Model for Nuclear Morphology and Stresses during Cell Transendothelial Migration. Biophysical Journal. 2016; 111(7):1541–1552. https://doi.org/10.1016/j.bpj.2016.08.011. PMID: 27705776
17. Schaefer A, te Riet J, Ritz K, Hoogenboezem M, Anthony EC, Mul FPJ, et al. Actin-binding proteins differentially regulate endothelial cell stiffness, ICAM-1 function and neutrophil transmigration. Journal of Cell Science. 2014; 127(20):4470–4482. https://doi.org/10.1242/jcs.154708 PMID: 25107367
18. Liu Z, Tan JL, Cohen DM, Yang MT, Sniadecki NJ, Ruiz SA, et al. Mechanical tugging force regulates the size of cell–cell junctions. Proceedings of the National Academy of Sciences. 2010; 107(22):9944–9949. https://doi.org/10.1073/pnas.0914547107
19. Schaefer A, Hordijk PL. Cell-stiffness-induced mechanosignaling–a key driver of leukocyte transendothelial migration. J Cell Sci. 2015; 128(13):2221–2230. https://doi.org/10.1242/jcs.163055 PMID: 26092932

20. Oldenburg J, de Rooij J. Mechanical control of the endothelial barrier. Cell and tissue research. 2014; 355(3):545–555. https://doi.org/10.1007/s00441-013-1792-6 PMID: 24519624

21. Ando K, Fukuhara S, Moriya T, Obara Y, Nakahata N, Mochizuki N. Rap1 potentiates endothelial cell junctions by spatially controlling myosin II activity and actin organization. J Cell Biol. 2013; 202(6):901–916. https://doi.org/10.1083/jcb.201301115 PMID: 24019534

22. Dorland YL, Huveneers S. Cell–cell junctional mechanotransduction in endothelial remodeling. Cellular and Molecular Life Sciences. 2017; 74(2):279–292. https://doi.org/10.1007/s00018-016-2325-8 PMID: 27506620

23. Huveneers S, Oldenburg J, Spanjaard E, van der Krogt G, Grigoriev I, Akhmanova A, et al. Vinculin associates with endothelial VE-cadherin junctions to control force-dependent remodeling. Journal of Cell Biology. 2012; 196(5):641–652. https://doi.org/10.1083/jcb.201108120 PMID: 22391038

24. Heemskerk N, Schimmel L, Oort C, Van Rijssel J, Yin T, Ma B, et al. F-actin-rich contractile endothelial pores prevent vascular leakage during leukocyte diapedesis through local RhoA signalling. Nature communications. 2016; 7. https://doi.org/10.1038/ncomms10493 PMID: 26814335

25. Galle J, Loeffler M, Drasdo D. Modeling the Effect of Deregulated Proliferation and Apoptosis on the Growth Dynamics of Epithelial Cell Populations In Vitro. Biophysical Journal. 2005; 88(1):62–75. https://doi.org/10.1529/biophysj.104.041459 PMID: 15475585

26. Fletcher AG, Osterfield M, Baker RE, Shvartsman SY. Vertex models of epithelial morphogenesis. Biophysical journal. 2014; 106(11):2291–2304. https://doi.org/10.1016/j.bpj.2013.11.4498 PMID: 24896108

27. Lin SZ, Li B, Xu GK, Feng XQ. Collective dynamics of cancer cells confined in a confluent monolayer of normal cells. Journal of Biomechanics. 2016; 52:140–147. https://doi.org/10.1016/j.jbiomech.2016.12.035 PMID: 28063647

28. Jamali Y, Azimi M, Mofrad MRK. A sub-cellular viscoelastic model for cell population mechanics. PLoS ONE. 2010; 5(8). https://doi.org/10.1371/journal.pone.0012097

29. Pathak A. Scattering of Cell Clusters in Confinement. Biophysical Journal. 2016; 111(7):1496–1506. https://doi.org/10.1016/j.bpj.2016.08.034 PMID: 27705772

30. Panorchan P, George JP, Wirtz D. Probing Intercellular Interactions between Vascular Endothelial Cadherin Pairs at Single-molecule Resolution and in Living Cells. Journal of Molecular Biology. 2006; 358(3):665–674. https://doi.org/10.1016/j.jmb.2006.02.021 PMID: 16540120

31. Yeh YT, Serrano R, François J, Chiu JJ, Li YSJ, del Álamo JC, et al. Three-dimensional forces exerted by leukocytes and vascular endothelial cells dynamically facilitate diapedesis. Proceedings of the National Academy of Sciences. 2017.

32. Burns AR, Walker DC, Brown ES, Thurmon LT, Bowden RA, Keese CR, et al. Neutrophil transendothelial migration is independent of tight junctions and occurs preferentially at tricellular corners. The Journal of Immunology. 1997; 159(6):2893–2903. PMID: 9300713

33. Guo M, Ehrlicher AJ, Jensen MH, Renz M, Moore JR, Goldman RD, et al. Probing the stochastic, motor-driven properties of the cytoplasm using force spectrum microscopy. Cell. 2014; 158(4):822–832. https://doi.org/10.1016/j.cell.2014.06.051 PMID: 25126787

34. Lecuit T, Yap AS. E-cadherin junctions as active mechanical integrators in tissue dynamics. Nature Cell Biology. 2015; 17(5):533–539. https://doi.org/10.1038/ncb3136 PMID: 25925582

35. Chen J, Newhall J, Xie ZR, Leckband D, Wu Y. A Computational Model for Kinetic Studies of Cadherin Binding and Clustering. Biophysical Journal. 2016; 111(7):1507–1518. https://doi.org/10.1016/j.bpj.2016.08.038 PMID: 27705773

36. Barry AK, Wang N, Leckband DE. Local VE-cadherin mechanotransduction triggers long-ranged remodeling of endothelial monolayers. Journal of Cell Science. 2015; 128(7):1341–1351. https://doi.org/10.1242/jcs.159954 PMID: 25663699

37. Yonemura S, Wada Y, Watanabe T, Nagafuchi A, Shibata M. α-Catenin as a tension transducer that induces adherens junction development. Nature Cell Biology. 2010; 12(6):533–542. https://doi.org/10.1038/ncb2055 PMID: 20453849

38. Suarez C, Kovar DR. Internetwork competition for monomers governs actin cytoskeleton organization. Nature Reviews Molecular Cell Biology. 2016; 17(12):799–810. https://doi.org/10.1038/nrm.2016.106 PMID: 27625321

39. Oldenburg J, De Rooij J. Mechanical control of the endothelial barrier. Cell and Tissue Research. 2014; 355(3):545–555. https://doi.org/10.1007/s00441-013-1792-6 PMID: 24519624

40. Sato M, Nagayama K, Kataoka N, Sasaki M, Hane K. Local mechanical properties measured by atomic force microscopy for cultured bovine endothelial cells exposed to shear stress. Journal of Biomechanics. 2000; 33(1):127–135. https://doi.org/10.1016/S0021-9290(99)00178-5. PMID: 10609525

41. Obenauf AC, Massagué J. Surviving at a Distance: Organ-Specific Metastasis. Trends in Cancer. 2015; 1(1):76–91. https://doi.org/10.1016/j.trecan.2015.07.009.

42. Krishnan R, Klumpers DD, Park CY, Rajendran K, Trepat X, van Bezu J, et al. Substrate stiffening promotes endothelial monolayer disruption through enhanced physical forces. American Journal of Physiology-Cell Physiology. 2011; 300(1):C146–C154. https://doi.org/10.1152/ajpcell.00195.2010 PMID: 20861463

43. Eguiluz RCA, Kaylan KB, Underhill GH, Leckband DE. Substrate stiffness and VE-cadherin mechanotransduction coordinate to regulate endothelial monolayer integrity. Biomaterials. 2017; 140:45–57. https://doi.org/10.1016/j.biomaterials.2017.06.010.

44. Jeon JS, Bersini S, Gilardi M, Dubini G, Charest JL, Moretti M, et al. Human 3D vascularized organotypic microfluidic assays to study breast cancer cell extravasation. Proceedings of the National Academy of Sciences. 2015; 112(1):214–219. https://doi.org/10.1073/pnas.1417115112

45. Chen MB, Whisler JA, Fröse J, Yu C, Shin Y, Kamm RD. On-chip human microvasculature assay for visualization and quantification of tumor cell extravasation dynamics. Nature Protocols. 2017; 12 (5):865–880. https://doi.org/10.1038/nprot.2017.018 PMID: 28358393

46. Osaki T, Sivathanu V, Kamm RD. Engineered 3D vascular and neuronal networks in a microfluidic platform. Scientific reports. 2018; 8(1):5168. https://doi.org/10.1038/s41598-018-23512-1 PMID: 29581463

47. Du X, Osterfield M, Shvartsman SY. Computational analysis of three-dimensional epithelial morphogenesis using vertex models. Physical biology. 2014; 11(6):066007. https://doi.org/10.1088/1478-3975/11/6/066007 PMID: 25410646

48. Okuda S, Inoue Y, Adachi T. Three-dimensional vertex model for simulating multicellular morphogenesis. Biophysics and physicobiology. 2015; 12:13–20. https://doi.org/10.2142/biophysico.12.0_13 PMID: 27493850

49. Alt S, Ganguly P, Salbreux G. Vertex models: from cell mechanics to tissue morphogenesis. Phil Trans R Soc B. 2017; 372(1720):20150520. https://doi.org/10.1098/rstb.2015.0520 PMID: 28348254

50. Tamulonis C, Postma M, Marlow HQ, Magie CR, de Jong J, Kaandorp J. A cell-based model of Nematostella vectensis gastrulation including bottle cell formation, invagination and zippering. Developmental Biology. 2011; 351(1):217–228. https://doi.org/10.1016/j.ydbio.2010.10.017. PMID: 20977902

51. Rejniak KA. An immersed boundary framework for modelling the growth of individual cells: An application to the early tumour development. Journal of Theoretical Biology. 2007; 247(1):186–204. https://doi.org/10.1016/j.jtbi.2007.02.019 PMID: 17416390

52. Sandersius SA, Newman TJ. Modeling cell rheology with the Subcellular Element Model. Physical biology. 2008; 5(1):15002. https://doi.org/10.1088/1478-3975/5/1/015002

53. Sandersius SA, Weijer CJ, Newman TJ. Emergent cell and tissue dynamics from subcellular modeling of active biomechanical processes. Physical Biology. 2011; 8(4):045007. https://doi.org/10.1088/1478-3975/8/4/045007 PMID: 21750367